Journal of Molecular Structure 1223 (2021) 129311

Contents lists available at ScienceDirect

Journal of Molecular Structure

journal homepage: www.elsevier.com/locate/molstr

Synthesis, characterization and *in-silico* assessment of novel thiazolidinone derivatives for cyclin-dependent kinases-2 inhibitors

Jasim Ali Abdullah[a], Bilal J M Aldahham[b], Muwafaq Ayesh Rabeea[b,*], Fatmah Ali Asmary[c], Hassna Mohammed Alhajri[c], Md Ataul Islam[d,e,f]

[a] Department of Chemistry, College of Education for Pure and Science, University of Mosul, Mosul, Iraq
[b] Department of Applied Chemistry, College of Applied Sciences-Hit, University Of Anbar, Hit 31007, Anbar, Iraq
[c] Chemistry Department, College of Science, King Saud University, P.O. Box 2455, Riyadh 11451, Saudi Arabia
[d] Division of Pharmacy and Optometry, School of Health Sciences, Faculty of Biology, Medicine and Health, University of Manchester, Oxford Road, Manchester M13 9PL, UK
[e] School of Health Sciences, University of Kwazulu-Natal, Westville Campus, Durban, South Africa
[f] Department of Chemical Pathology, Faculty of Health Sciences, University of Pretoria and National Health Laboratory Service Tshwane Academic Division, Pretoria, South Africa

ARTICLE INFO

Article history:
Received 9 August 2020
Revised 17 September 2020
Accepted 19 September 2020
Available online 22 September 2020

Keywords:
CDK2
Grinding
Thiazolidinone
Molecular docking
Pharmaceutical chemistry

ABSTRACT

This work aims to synthesize thiazolidinone derivatives using a rapid, safe and solvent-free grinding assisted approach. The newly synthesized compounds have been targeted due to their bioactivity in wide pharmaceutical uses, especially, as anti-proliferative agents. Two thiazolidinone derivatives having a diverse set of crucial functional groups were diagnosed with melting point (m.p), FT-IR, ^{1}H NMR, ^{13}C NMR, GC-Mass and CHNS. High outputs (98% and 96%) of thiazolidinone derivatives were offered by the grinding method and the final product was produced over short reaction times (5 min). This simple strategy would potentially be promising for the preparation of thiazolidinone derivatives in abundance. Followed by synthesis both of our molecules were considered for molecular docking study against the Cyclin-Dependent Kinase 2 (CDK2) protein. A number of potential binding interactions in terms of hydrogen and hydrophobic bonds were observed with the ligand-binding amino acid of CDK2 protein. The behavior of both molecules inside the CDK2 was explored through all-atoms molecular dynamics (MD) simulations. Several parameters calculated from the MD simulation were revealed that both molecules retained inside the receptor cavity of CDK2. Hence, green synthesized both compounds were found to show strong potentiality against the CDK2 and may have significant interests in the field of pharmaceutical chemistry.

© 2020 Elsevier B.V. All rights reserved.

1. Introduction

Heterocyclic compounds are the aromatic and/or cyclic molecules consisting of several heteroatoms in the rings included nitrogen, sulfur, oxygen, etc. [1]. The heterocyclic compounds are pharmaceutically important but still a lot of information about it yet to solve [2,3]. Most of the plant extracts are comprising of heterocyclic rings as heterocycles form the core structures for mono and polysaccharides and the DNA sequence bases that make up the genetic code [4–6]. A number of crucial pharmaceuticals are made up of heterocyclic molecules [7,8]. Chemical and physical properties contribute to improved bioavailability and versatility relative to heterocyclic aromatic hydrocarbons [9–11]. The solubility in water and polarity of heterocyclic compounds is depends on the replacement of a single carbon atom with oxygen, nitrogen, or sulfur [1,12].

Thiazolidinones are one of the most important heterocyclic compounds whose derivatives, having a carbonyl group in fourth place, an essential part of numerous synthetic pharmaceuticals with a wide variety of biological activities [13,14] including anticancer, antihyperlipidemic, antiparasitic and monoamine oxidase inhibitor [15–19]. Microwave and ultrasonic irradiation are used to synthesize a variety of heterocyclic compounds, resulting in the acceleration of chemical reactions without the use of organic solvents [20–23].

Cyclin-dependent kinases-2 (CDK2) is a type of kinase group (CKDs) of the protein responsible of control the cell-cycle progression by activation of the phosphorylating proteins in serine/threonine as the site of binding, involved in cell division [24]. The CDK2 is approved in literature, has a critical role in tumor development in several types of cancer [25–29], and the targeting

* Corresponding author.
E-mail address: muw88@uoanbar.edu.iq (M.A. Rabeea).

https://doi.org/10.1016/j.molstruc.2020.129311
0022-2860/© 2020 Elsevier B.V. All rights reserved.

of CDK2 by inhibiting it is a high efficacy strategy of predicting the activity of anti-tumor agents. Thiazolidinone based derivatives showed vigorous anticancer activity with infinitesimal concentrations (nanomolar range) [30–32].

A number of CDK2 inhibitors included Flavopiridol [33], Roscovitine [34], Dinaciclib [35], SNS032 [36], AT7519 [37] and Milciclib [38] are entered in the different stages of clinical trials [39]. It is important to note that Flavopirido, Roscovitine, AT7519 and Milciclib are in clinical trial stage II. The Dinaciclib and SNS032 are in clinical trials III and I respectively. A two-dimensional representation of the above CDK2 inhibitors are given in Table S1 (Supplementary data). All the above inhibitors show biological efficacy in a number of diseases included tumorigenesis.

Many studies were focused on the preparation of some heterocyclic compounds using the grinding method [40–45], however, as far as we know, there is no mention of the synthesis of thiazolidinone derivatives from Schiff bases by the use of grinding throughout the entire production process. Hence, this work deems the new attempt to synthesize two important pharmaceutical thiazolidinone derivatives by grinding-assisted. Continuously, this protocol would offer a great incentive to make it easy to synthesize a wide range of new thiazolidinone derivatives. After successful synthesis two compounds were used for *in-silico* assessment included molecular docking and molecular dynamics (MD) simulation studies. Therefore, the prediction of CDK2 successful inhibitors among the family of thialozidinone derivatives, the promising anticancer group, and seeking the bioactivity of newly synthesized compounds is the aim of this work.

2. Materials and methods

2.1. Grinding assisted synthesis

The 4-amino antipyrine (0.01 mole) has been used to synthesize the Schiff bases (Sch-I and Sch-II) by grinding. It was ground once together with 3-hydroxybenzaldehyde (0.01 mole) and again with 4-nitrobenzaldehyde (0.01 mole) by porcelain mortar for 5–10 min respectively. Following a few minutes of grinding, the blend becomes a wet, homogenized substance with a change of color. During the grinding process, 15 mL of diethyl ether was added. Finally, the precipitant output was washed, dried, and recrystallized with absolute ethanol [46].

To synthesis compound 1(Comp1), a mixture of Sch-I (0.001 moles) and thioglycolic acid (0.001 mole) has been ground in a mortar with a pestle made of porcelain for 5 min (Scheme 1). After 2 min of grinding, the blend is an organic kneading with a change of color during the machining process. The output was eventually filtered, dried, and recrystallized by T.H.F. [47]. Thioglycolic acid (0.001 mole) was mixed with Sch-II (0.001 mole) for synthesis compound 2 (Comp2) under the same conditions as those described above.

2.2. Characterization of synthesis product

All organic compounds and solvents were obtained from Sigma-Aldrich and all analyses have been carried out at the University of Rostock, Germany. Stuat melting apparatus (SM30) has been used to determine the melting point. Bruker AC 250, Bruker ARX 300 and Bruker ARX 500 have been used to record ^{1}H NMR and ^{13}C NMR spectra. All ^{1}HNMR and ^{13}C NMR spectra provided in this analysis were obtained in either CDCl3 or DMSO–d6. Both chemical changes are performed in ppm. TMS was used as an internal source. A Bruker FT-IR Spectrophotometer (Tensor 27 Germany) and a biotech Engineering FT-IR-600 (UK., using KBr discs, Alpha Bruker/ATR Diamond) was used to perform infrared spectra.

Mass spectrometry (MS) was investigated using AMD MS40, Varian MAT CH7, MAT 731 (EI, 70ev), intecta AMD 402 (EI, 70ev, and CI), Finnigan MAT 95 (CI, 200ev). Varian MAT 311, Intecta AMD 402 was used to record High-Resolution Mass Spectrometry (HRMS). To Elemental Analysis, Thermoquest Flash EA 1112 (LECO CHNS-932) has been used. Thin-layer chromatography (TLC) was performed in the presence of iodine as an aspect of the spot.

Characterization of Sch-I (Figures S1-S4 in supplementary file**);** Yield%: 96. White crystals. m.p: 280–282 °C. Rf: 0.6. FT-IR (KBr), ν (cm^{-1}): 1622 (C=O), 1605 (CH=N), 1580 (C=C), 3156 (O–H). ^{1}H NMR (25 °C, $CDCl_3$): 2.12 (s, C–CH_3), 3.13 (s, N–CH_3), 9.48 (s, CH=N), 9.46 (s.br, OH), 7.13–7.51 (m, 9H, Ar-H). ^{13}C NMR (25 °C, $CDCl_3$): 9.97 (C-*CH_3), 35.33 (N-*CH_3), 105.23–136.73 (CH_3-*C=*C-N), 153.21 (CH_2, C–OH), 157.7 (*CH.CH=N), 116–147 (Ar-C), 160.33 (C=O). Mass, *m/z* (%): 308 (16), 307 (75), 199 (23), 188 (25), 171 (19), 121 (33), 89 (15), 77 (17), 56 (100), mol. mass (307.132). CHNS: ($C_{18}H_{17}N_3O_2$) 70.130 (C_{theo}), 70.230 (C_{prac}), 5.580 (H_{theo}), 5.680 (H_{prac}), 13.670 (N_{theo}), 13.880 (N_{prac}).

Characterization of Sch-II (Figures S5-S8 in supplementary file**);** Yield%: 98. Orange. m.p: 260–261 °C. Rf: 0.7. FT-IR (KBr), ν

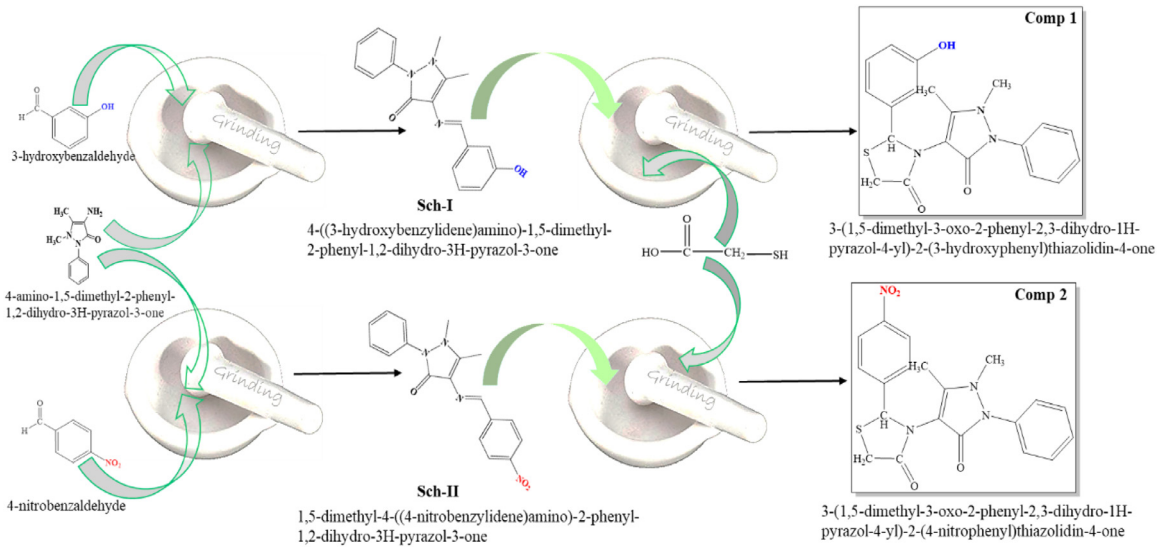

Scheme 1. Steps synthesis of Comp1 and Comp2.

(cm^{-1}): 1641 (C=O), 1596 (CH=N), 1572 (C=C). ^{1}H NMR (25 °C, $CDCl_3$): 2.43 (s, C–CH_3), 3.15 (s, N–CH_3), 9.52 (s, CH=N), 7.21–8.43 (m, 10H, Ar-H). ^{13}C NMR (25 °C, $CDCl_3$): 10.12 (C-*CH_3), 34.87 (N-*CH_3), 109.83–135.97 (CH_3–*C*=C–N), 159.8 (*CH.CH=N), 122–152 (Ar-C), 161.47 (C=O). Mass, *m/z* (%): 337 (6), 336 (34), 188 (20), 121 (33), 91 (22), 78 (14), 44 (13), mol. mass (336.122). CHNS: ($C_{18}H_{16}N_4O_3$) 64.280 (C_{theo}), 64.470 (C_{prac}), 4.790 (H_{theo}), 4.810 (H_{prac}), 16.660 (N_{theo}), 16.750 (N_{prac}).

Characterization of Comp 1 (Figures Fig. S9-S12 in supplementary file**);** Yield%: 96. Pale Yellow. m.p: 170–172 °C. Rf: 0.55. FT-IR (KBr), ν (cm^{-1}): 1687, 1642 (C=O), 1597 (C=C), 670 (C-S), 3156 (O–H). ^{1}H NMR (25 °C, $CDCl_3$): 2.01 (s, C–CH_3), 3.04 (s, N–CH_3), 2.85–4.08 (q, 2H, CH_2), 9.46 (s.br, OH), 6.12 (s,C–H), 6.85–7.55 (m, 9H, Ar-H). ^{13}C NMR (25 °C, $CDCl_3$): 10.80 (C-*CH_3), 35.26 (N-*CH_3), 107.18–137.22 (CH_3–*C*=C–N), 31.65, 152.34 (CH_2, C–OH), 61.56 (*CH.CH=N), 115–151 (Ar–C), 167.45 (C=O AP), 170.22 (C=O Lactam). Mass, *m/z* (%): 382 (16), 381 (79), 348 (13), 306 (31), 246 (16), 215 (54), 188 (100), 137 (13), 121 (65), 56 (77), mol. mass (381.115). CHNS: ($C_{20}H_{19}N_3O_3S$) 62.97 (C_{theo}), 62.829 (C_{prac}), 5.02 (H_{theo}), 5.294 (H_{prac}), 11.02 (N_{theo}), 11.211 (N_{prac}), 8.41 (S_{theo}), 8.443 (S_{prac}).

Characterization of Comp 2 (Figures S13-S16 in supplementary file**);** Yield%: 98. Green. m.p: 79–80 °C. Rf: 0.53. FT-IR (KBr), ν (cm^{-1}): 1725, 1642 (C=O), 1596 (C=C), 699 (C-S). ^{1}H NMR (25 °C, $CDCl_3$): 2.44 (s, C–CH_3), 3.16 (s, N–CH_3), 2.76–3.93 (q, 2H, CH_2), 6.03 (s, C–H), 7.35–8.51 (m, 9H, Ar-H). ^{13}C NMR (25 °C, $CDCl_3$): 10.01 (C-*CH_3), 35.79 (N-*CH_3), 105.22–135.11 (CH_3-*C=*C-N), 33.73 (CH_2, C–OH), 64.17 (*CH.CH=N), 119–148 (Ar-C), 161.35 (C=O AP), 170.17 (C=O Lactam). Mass, *m/z* (%): 411 (24), 410 (69), 372 (15), 371 (73), 330 (19), 329 (29), 238 (41), 203 (15), 189 (79), 188 (55), mol. mass (410.105). CHNS: ($C_{20}H_{18}N_4O_4S$) 58.530 (C_{theo}), 58.481 (C_{prac}), 4.42 (H_{theo}), 4.416 (H_{prac}), 13.65 (N_{theo}), 13.643 (N_{prac}), 7.81 (S_{theo}), 7.821 (S_{prac}).

2.3. Molecular docking

Molecular docking is one of the crucial *in-silico* approaches to predict the preferred binding orientation of the small molecule inside the receptor cavity of the macromolecule. Synthesized two molecules (Comp1 and Comp2) were docked in the CDK2 protein molecule using the AutoDock vina (ADV) [48]. The crystal structure of the CDK2 was collected from the Research Collaboratory for Structural Bioinformatics-Protein Data Bank (RCSB-PDB) with PDB ID: 3FZ1 [49]. The resolution and R-value of the selected CDK2 protein are found to be 1.90 Å and 0.210 respectively. The protein consisted of a single chain having a total of 298 amino residues. Prior to molecular docking the CDK2 crystal structure was prepared using the AutoDock tools (ADT) [50]. The crystal water molecules were deleted. The polar hydrogens and charges were added. The protein atoms were assigned the AD4 (Autodock 4) type and saved as pdbqt format. The grid coordinates were set as 1.448, 25.918 and 9.073 along X-, Y- and Z-axes respectively. The grid box size was set to 40×40×40 along the X-, Y- and Z-axes respectively. Both compounds were also prepared using ADT. The hydrogens and Gasteiger charges were added. The number of torsions was set and default docking parameters were considered. Both molecules were saved as pdbqt file format for the molecular docking input in ADV. After successful docking, the binding energy was recorded and binding interactions were analysed using the Protein-Ligand Interaction Profiler (PLIP) [51] online server.

2.4. Molecular dynamics simulation

Molecular dynamics (MD) simulation is an excellent approach to explore the dynamic structural information on biomacromolecules. Moreover, it is also crucial to analyze the energetic information about protein and ligand interactions. The structural behavior of novel thiazolidinone compounds complex with CDK2 protein in dynamic states was explored through an all-atoms MD simulation for a 100 ns period. Individual docked complex of Comp1 and Comp2 with CDK2 were considered. The simulation was performed in the Amber18 [52] software package installed at the Computational Shared Facility (CSF3), University of Manchester, UK. Each complex was immersed in truncated octahedron of TIP3P [53] water prior to the simulation. To neutralize the system a required number of Na+ and Cl- were added and maintained the ionic strength of 0.1 M to mimic the physiological pH. The protein topology was generated through the ff14SB force field [54]. The Nvidia V100-SXM2–16GB Graphic Processing Unit using the PMEMD.CUDA [55] module was used to execute the simulation. In the simulation, the temperature of 300 K was maintained through the Langevin thermostat with a collision frequency of 2 ps-1, at 1 atm using a Monte Carlo barostat with volume exchange attempts every 100 fs. Moreover, a 2-fs integration step was retained. The SHAKE [56] algorithm was used to constrain the hydrogens involved in covalent bond. For the short-range nonbonded interaction the cut-off was set to 8 Å and the long-range electrostatics were preserved through the particle mesh Ewald method. A total of 10 ns equilibration was performed consisting of rounds of NVT and NPT. A number of parameters included root-mean-square deviation (RMSD) of CDK2 backbone and ligands, root-mean-square fluctuation (RMSF) and radius of gyration (RoG) were explored using CPPTRAJ [57] over full trajectory, taking configuration every 2 ps.

2.5. Binding free energy calculation through MM-GBSA approach

The molecular mechanics-generalized born surface area (MM-GBSA) approach to calculate the binding free energy (ΔG_{bind}) of any small molecule is considered to be more accurate and widely accepted in the scientific community. This approach quantitively measures the binding potency between the protein and small molecules. The ΔG_{bind} of both molecules was calculated from the post-processed ensemble of structures obtained from the MD simulation trajectories. The ΔG_{bind} calculation using the MM-GBSA approach was carried out through the following expressions.

$$\Delta G_{bind} = G_{com} - \left(G_{rec} + G_{lig}\right) \tag{1}$$

$$\Delta G_{bind} = \Delta H - T\Delta S \tag{2}$$

$$\Delta G_{bind} = \Delta E_{MM} + \Delta G_{sol} - T\Delta S \tag{3}$$

$$\Delta E_{MM} = \Delta E_{int} + \Delta E_{ele} + \Delta E_{vdw} \tag{4}$$

$$\Delta G_{sol} = \Delta G_{pol} + \Delta G_{npol} \tag{5}$$

The total binding energy (ΔG_{bind}) is obtained (Eq. (1)) by the difference of free energy between complex (ΔG_{com}) and summation of the receptor (ΔG_{rec}) and ligand (ΔG_{lig}). Further, the ΔG_{bind} is consisting of two terms, enthalpy (ΔH) and entropy (TΔS). The enthalpy term is calculated using the GBSA, and entropy is obtained from the normal mode analysis (NAM) and interaction entropy (IE) approaches. The ΔH can be represented by molecular mechanical energy (ΔE_{MM}) and solvation free energy (ΔE_{sol}). The ΔE_{MM} is the summation of intra-molecular (ΔE_{int}), electrostatic (ΔE_{ele}) and the van der Waals interaction (ΔE_{vdw}) energies. Further, the free energy of solvation (ΔG_{sol}) can be expressed by the summation of polar (ΔG_{pol}) and non-polar (ΔG_{npol}) energies. The modified generalized Born (GB) [58] is used to calculate the ΔG_{pol} and ΔG_{npol} obtained from the LCPO algorithm [59] which is based on SASA.

3. Result and discussion

The use of organic solvents in different chemical reactions is harmful both to the environment and to human health. As a result, numerous methods have emerged in the synthesis of organic materials. Green chemistry depends on the absence of chemical solvents, and use of simple procedures, the shortening of time reactions and excellent yields. Here, grinding-assisted reactions between 4-amino antipyrine and substituted benzaldehydes were used to synthesize a 4-(3–hydroxy benzylidene amino) antipyrine (Sch-I) and 4-(4-nitro benzylidene amino) antipyrine (Sch-II) at room temperature. The preparation of the Schiff bases compounds taking 5 min for Sch-I with a yield of 96%, which contains an OH group. Sch-II containing NO_2 group is obtained through 10 min with a yield of 98%. The variation of color, melting point and TLC of the raw material after the synthesis process is the initial signs of a completed chemical reaction.

For the synthesis of Schiff bases and thiazolidinone derivatives, two precursors with different functional groups of withdrawing group (NO_2) and donating group (OH) were used. The use of the grinding strategy did not involve catalysing by adding mineral acid (H^+) during the preparation of the Schiff bases, making the nucleophilic attack easier. The NO_2 group led to creating a huge positive charge on the carbon atom of the carbonyl group, which facilitates interaction with the nucleophile and shows higher product compared to the OH group. The Sch-I and Sch-II synthesis mechanism (Scheme 2) indicates that the electron pair of amine group attacks (nucleophilic attack) carbon of the aldehyde carbonyl group [60]. This leads to formation intermediate compounds (4-((hydroxy(3-hydroxyphenyl)methyl)amino)−1,5-dimethyl-2-phenyl-1,2-dihydro-3H-pyrazol-3-one and 4-((hydroxy(4-nitrophenyl)methyl)amino)−1,5-dimethyl-2-phenyl-1,2-dihydro-3H-pyrazol-3-one) which then lose the water molecule and become stable amine compounds.

The FT-IR spectra for Sch-I and Sch-II show peaks (1605–1596 cm^{-1}) associated with the azomethine group. Other peaks (1622–1641 cm^{-1}) and (1580–1572 cm^{-1}) corresponded to the carbonyl and aromatic groups respectively. Sch-I was distinguished by a peak at (3165 cm^{-1}) due to the (OH) group. ^1H NMR spectra of Sch-I and Sch-II show a chemical shift in 9.48–9.51 ppm assigned to (CH = N) while Sch-I reveals a singlet peak at 9.46 ppm associated with Ar-OH. ^{13}C NMR spectra appear major peaks at 157.7 ppm and 159.8 ppm related to carbon in CH_3–C=N. Sch-I shows a peak at 153.21 associated with CH_2–C–OH [61]. The Sch-I and Sch-II mass spectra have been registered, and the *m/z* value obtained of the new compounds matched the theoretical molecular weight of the compounds. The purities of Sch-I and Sch-II were evaluated by elementary analysis.

The synthetic route for the target thiazolidine derivatives (comp 1 and comp 2) was carried out as illustrated in Scheme 1. Sch-I was reacted with thioglycolic acid by grinding for 5 min without solvent. Comp 2 was synthesized under the same method conditions by the reaction of Sch-II with thioglycolic acid. Scheme 3 is a proposed mechanism for the synthesis of thiazolidine derivatives. Describing the synthesis mechanisms of Comp 1 and Comp 2, a nucleophilic attack by the electron pair of the sulfur atom in thioglycolic acid attacked the carbon atom at the Schiff's bases. Continuously, the electron pair on the nitrogen of Schiff's bases triggers a nucleophilic attack on the carbon atom of the carboxyl group [60,62].

The chemical structure of the synthesized derivatives thiazolidine (Comp 1 and Comp 2) was interpreted by ^1H NMR, ^{13}C NMR, GC-Mass and CHNS spectra. In FT-IR spectra, the focus was on the major peak at 1166 cm^{-1} related to the C-S-N group which appeared in comp1 and comp2 compared to the compounds of their Schiff bases (Sch-I and Sch-II) [61].

The ^1H NMR spectra of comp1 and comp2 have illustrated all the protons of synthesized compounds. There is a chemical shift at 9.46 ppm due to proton of OH in comp1 that is not found in comp2 because OH is replaced by NO_2. While the chemical shifts at 9.48 −9.52 ppm(s) for proton in Schiff bases have been disappeared because of the formation of the thiazolidine group (CH=N). There is another indicator of the formation of thiazolidinone compounds from the corresponding Schiff bases, depending on the ^{13}C NMR spectra. The presence of a new shift at 60–64 ppm assigned to C-S (newly formed) of comp1 and comp2, as well as a shift at 170 ppm indicating the formation of a new cyclic moiety in molecules.

GC-Mass spectra of synthesized compounds were recorded. All molecular mass indicates the possible breakdown in the chemical composition of the compound is prepared. The final result appears a molecular ion peak at *m/z* = 188 assigned to the (N–N–C=O)

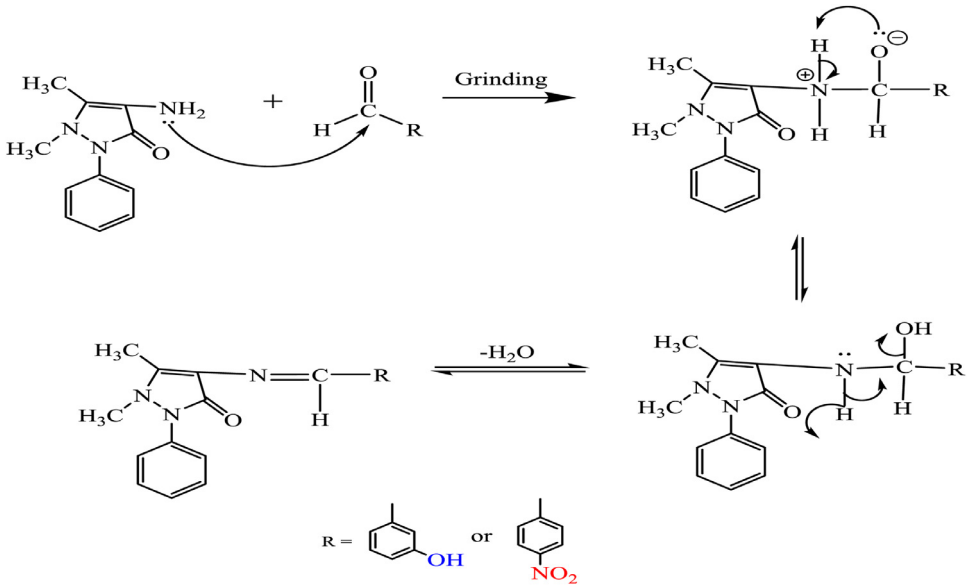

Scheme 2. mechanism of Schiff base (Sch-I and Sch-II) preparation.

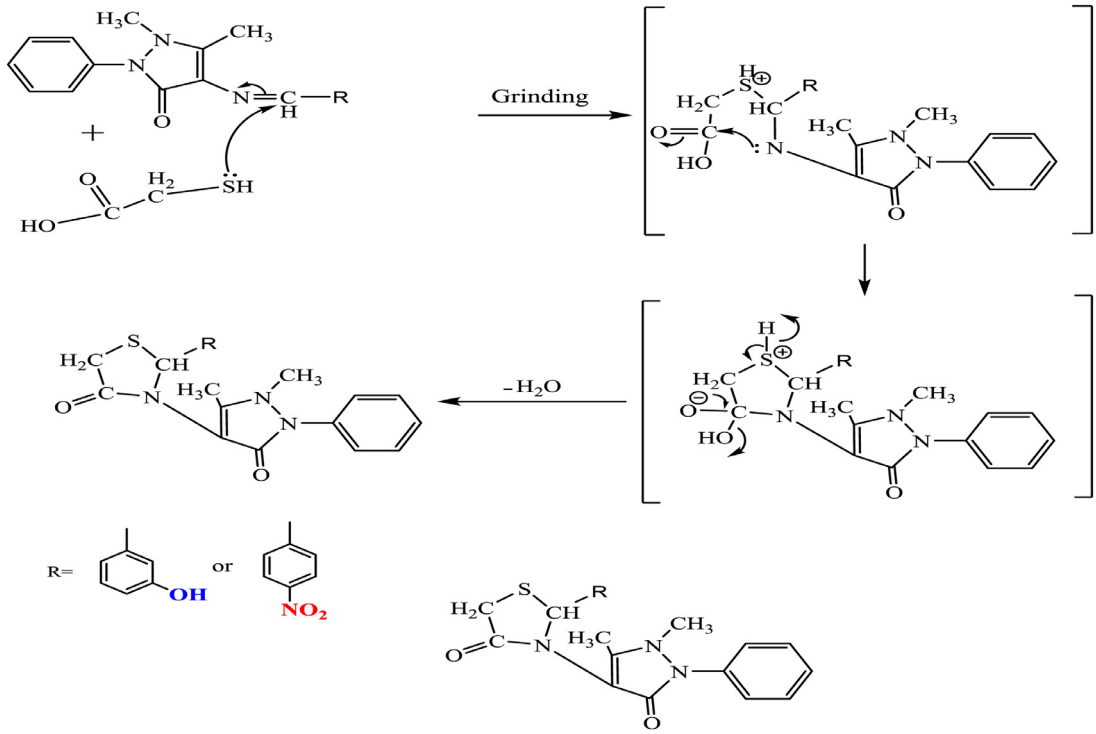

Scheme 3. A possible mechanism to prepare Comp1 and Comp2.

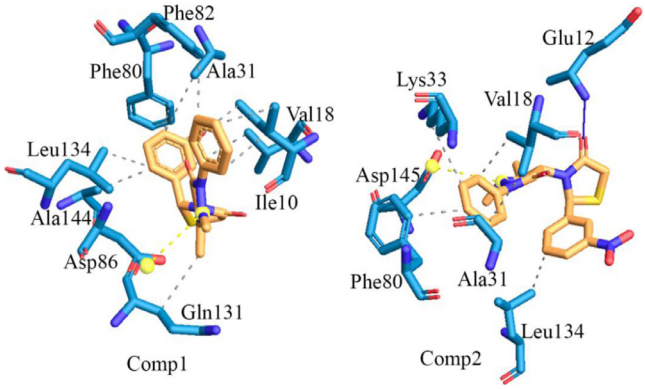

Fig. 1. Binding interactions profile of Comp1 and Comp2.

group. The description of CHNS data has been shown to be compatible with the basic elements of our compounds.

3.1. Molecular docking

Molecular docking of both compounds (Comp1 and Comp2) was uncovered that both fit well into the coupling site and show great communications with the critical amino corrosive build-ups. To approve the docking conventions of the binding site of CDK2, the molecular docking experiment was performed in the ADV tool and the binding interactions were visualized in the PLIP online server. The binding energy was found to be −8.7 and −8.1 Kcal/mol for Comp1 and Comp2 respectively. The binding interaction profile of Comp1 and Comp2 is given in Fig. 1.

From binding interactions analysis, it can be seen that the amino acid residues, Ile10, Val18, Ala31, Phe80, Phe82, Gln131, Leu134, and Ala144 were found to be interacted with Comp1 through hydrophobic interactions. Moreover, a salt bridge was also found between Comp1 and Asp86. Comp2 was found to establish a hydrogen bond with Glu12. In addition to the above a number of amino residues included Val18, Ala31, Lys33, Phe80 and Leu134 were interacted with Comp2 via hydrophobic interactions. The binding mode of both compounds was checked in a three-dimensional surface view and it is given in Fig. 2. It can be seen that both compounds perfectly fitted almost the same position of CDK2 receptor.

A set of six standard CDK2 inhibitors (Flavopiridol, Roscovitine, Dinaciclib, SNS032, AT7519 and Milciclib) [39] were collected and docked in the CDK2 to explore the binding energy and binding interactions. The two-dimensional structure along with inhibitory activity and binding energy of all inhibitors are given in Table S1 (Supplementary file). The binding energy of Flavopiridol, Roscovitine, Dinaciclib, SNS032, AT7519 and Milciclib was found to be −8.30, −7.90, −8.50, −7.80, −8.20 and −9.90 Kcal/mol respectively. Hence, it is clear that Comp1 (−8.7 Kcal/mol) possessed a higher binding affinity towards CDK2 in comparison to all standard CDK2 inhibitors except Milciclib. Comp2 was found to show higher affinity compared to Roscovitin and SNS032. The binding energy of other CDK2 inhibitors except Milciclib was found to be comparable with Comp2. The binding interactions of all standard CDK2 inhibitors were assessed and it is given in Figure S17 (Supplementary data). It is important to note that a number of ligand-interacting amino acids were found common to the standard CDK2 inhibitors and, Comp1 and Comp2. Therefore, above analyses clearly indicated that both synthesized molecules (Comp1 and Comp2) might be potential as of already available standard CDK2 inhibitors.

3.2. Pharmacokinetic analysis

The pharmacokinetic and physicochemical properties are important to explore the potentiality of the newly synthesized compounds. The SwissADME, an online server was used to calculate the pharmacokinetic and physicochemical characteristics of both Comp1 and Comp2 and these are given in Table 1. The relative molecular mass of Comp1 and Comp2 was found to be 381.45 and

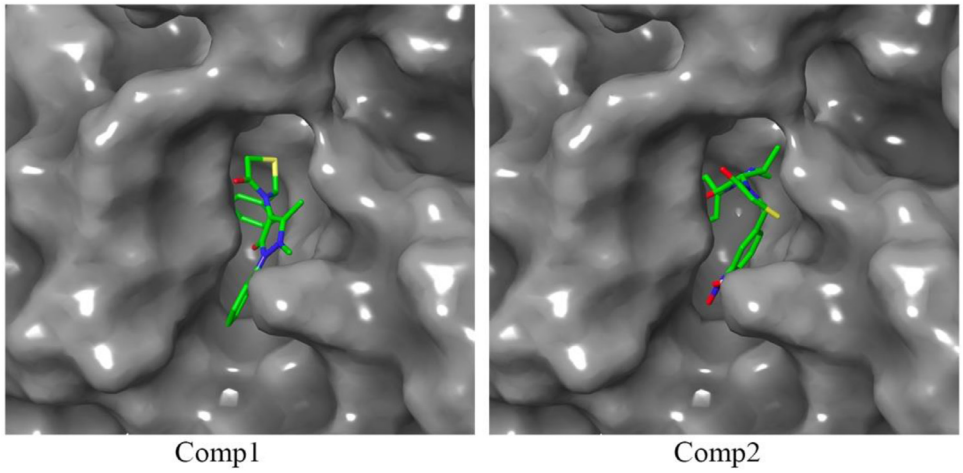

Fig. 2. Binding mode of Comp1 and Comp2 in the CDK2.

Table 1
Pharmacokinetic and physicochemical properties of Comp1 and Comp2.

Parameters	Comp1	Comp2
Formula	$C_{20}H_{19}N_3O_3S$	$C_{20}H_{18}N_4O_4S$
[a]MW	381.45 g/mol	410.45 g/mol
[b]NHA	27	29
[c]NAHA	17	17
[d]NRB	3	4
[e]MR	110.39	117.19
[f]TPSA (Å^2)	92.77	118.36
[g]LogS	−4.54	−4.73
[h]SC	Moderately soluble	Moderately soluble
[i]GI	High	High
[j]BBB	No	No
[k]vROF	0	0
[l]vGhose	0	0
[m]vVeber	0	0
[n]BS	0.55	0.55
[o]SA	3.74	3.87
LogP	2.62	2.37

[a] Molecular weight.
[b] No. of heavy atoms.
[c] No.of aromatic heavy atoms.
[d] No. of rotatable bonds.
[e] Molar refractivity.
[f] Topological polar surface area.
[g] Solubility.
[h] Solubility class.
[i] Gastrointestinal absorption.
[j] Blood Brain Barrier Penetration.
[k] Violation of Lipinski's rule of five.
[l] Violation of Ghose rule.
[m] Violation of Veber rule.
[n] Bioavailability Score.
[o] Synthetic accessibility.

410.45 g/mol, respectively. Oral activeness is explained by the value of TPAS. The newly synthesized compounds were found to have 92.77 and 118.36 for Comp1 and Comp2 respectively, which indicates that they are orally active. The criteria of drug-likeness are derived from Lipinski's rule of five, Ghosh's and Veber's rule. Both compounds were found to follow the above drug-likeness rules perfectly. Both molecules are moderately soluble in nature. The absorption in the gastrointestinal (GI) tract was found to be high for both molecules. Low synthetic accessibility value was clearly indicated that both molecules not difficult to synthesis. Hence, the above data undoubtedly favours the potentiality of the molecules.

Table 2
RMSD, RMSF, RoG and binding free energy of Comp1 and Comp2.

			Maximum	Minimum	Average
RMSD (Å)	Protein backbone	Comp1	2.601	0.000	2.100
		Comp2	2.592	0.000	1.965
	Ligand	Comp1	3.100	0.000	1.176
		Comp2	2.878	0.000	1.265
RMSF (Å)		Comp1	4.633	0.371	0.842
		Comp2	3.742	0.386	0.901
RoG (Å)		Comp1	20.186	19.602	19.907
		Comp2	20.161	19.492	19.781
Binding energy (Kcal/mol)			Ele.	vwd.	ΔG_{bind}
		Comp1	−29.035	−43.242	−35.094
		Comp2	51.736	−46.135	−32.796

Ele. = Electrostatic; vwd: van der Waals.

3.3. Molecular dynamics simulation

In the drug discovery research, a combined approach of molecular docking and MD simulation studies became a pivotal method among the scientific community in academia and industry. In this regard, both Comp1 and Comp2 were docked in the CDK2 and subsequently considered for 100 ns MD simulation. After successful completion of the simulation, a number of parameters included RMSD, RMSF, RoG and binding free energy were calculated and these are given in Table 2.

The RMSD of each frame of CDK2 backbone bound with Comp1 and Comp2 was calculated and it is given in Fig. 3. It can be seen that initially the RMSD value of CDK2 backbone bound with both Comp1 and Comp2 was gradually increased. In the case of CDK2- Comp2 complex, the system was achieved stability after about 10 ns. On the other hand, the backbone of CDK2 bound with Comp1 was found to have fluctuation initially but after about 40 ns it was achieved perfect stability till the end of the simulation. The average RMSD value also can give an idea about the stability of the protein backbone during the simulation. The average RMSD of CDK2 backbone bound with Comp1 and Comp2 was found to be 2.100 and 1.965 Å respectively. Hence, low average RMSD and consistent variation of backbone undoubtedly explained the stability of protein-ligand complexes.

The RMSD of both Comp1 and Comp2 was obtained and it is given in Fig. 4. It was observed that ligand RMSD was varied from 0 to 3.100 Å. The RMSD of Comp1 was found to be consistent throughout the simulation except for a small fluctuation around 45 ns of simulation time. Comp 2 was shown a small fluctuation and remained intact during the simulation. No significant fluctu-

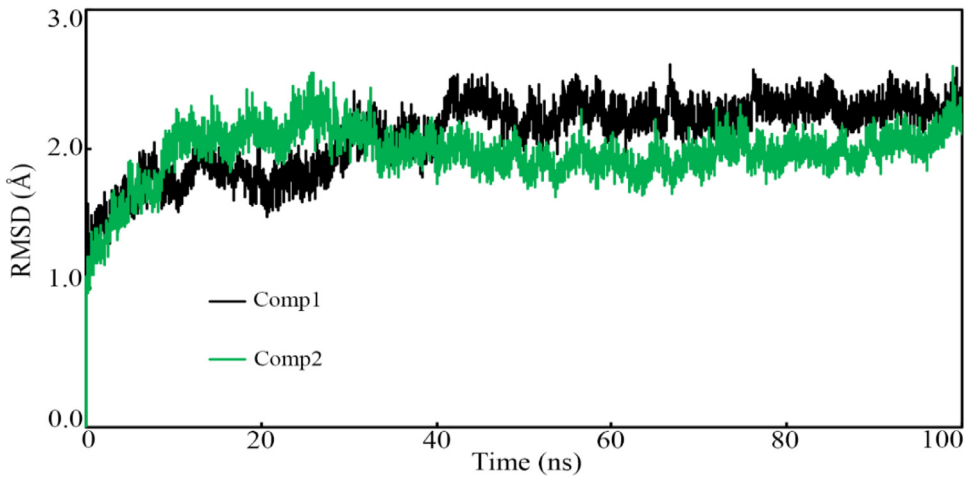

Fig. 3. RMSD of CDK2 backbone bound with Comp1 and Comp2.

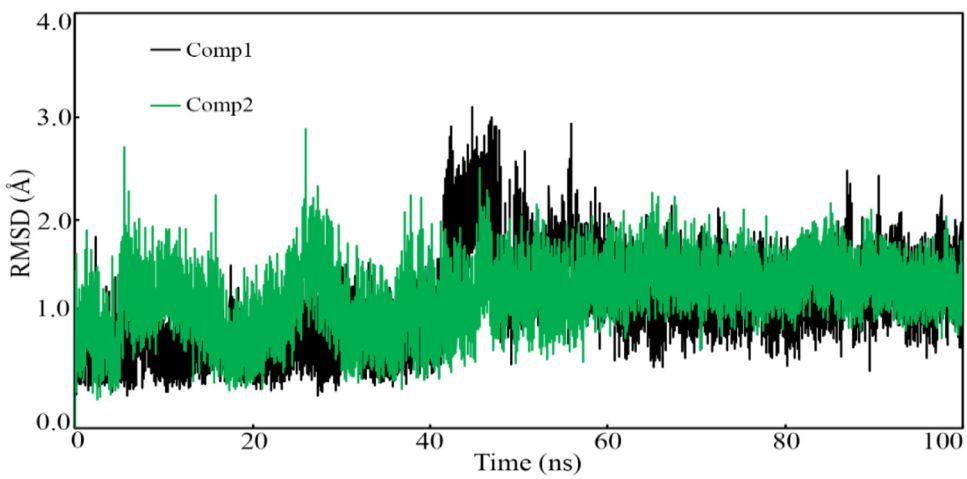

Fig. 4. RMSD of Comp1 and Comp2 during MD simulation.

ation was observed. The difference between the maximum and average RMSD can explain the deviation of the molecules from its mean position. In the case of Comp1 and Comp2 the difference between the maximum and average RMSD value was found to be 1.924 and 1.613 Å respectively. The above data clearly suggested that both molecules remained inside the pocket without any higher conformational changes.

RMSF of individual amino residue is an important parameter to explore the stability of protein-ligand complexes. This parameter tells about the fluctuation of each amino acid which dealings the average divergence of each amino acid from the reference position. The RMSF of the individual amino residue of CDK2 bound with Comp1 and Comp2 was calculated from the MD simulation trajectory and it is given in Fig. 5. It is important to note that the variation of RMSF was found to be more or less similar for both Comp1 and Comp2. The highest RMSF value was found for Gly146 and His147 when bound with Comp1 and Comp2 respectively. The above observation might be due to lack of binding interaction with a ligand or the presence of both amino residues in the flexible region of the CDK2. The average RMSF was found to be 0.842 and 0.901 in the case of CDK2 bound with Comp1 and Comp2 respectively.

The compactness of the system during the MD simulation can be assessed through RoG. RoG of both complexes was calculated and it is given in Fig. 6. Consistent variation of RoG indicates the stably folding of protein during the MD simulation. The high fluctuation of the RoG parameters described the unfolding the protein over the time of the simulation. In the current study, extremely less variation of CDK2 was observed for both cases of Comp1 and Comp2. The difference between the highest and lowest RoG of CDK2 was found to be 0.584 and 0.669 Å when bound with Comp1 and Comp2 respectively. The above low value and consistent plot of RoG clearly explained that both the complexes were compact during the simulation.

In order to explore the binding affinity of both Comp1 and Comp2 towards the CDK2, the binding free energy was calculated through MM-GBSA approach. The binding free energy obtained from the MM-GBSA is widely accepted and explored by the scientific community and also thought to be more authentic in contrast to molecular docking based binding energy [63–65]. The ΔG_{bind} of both Comp1 and Comp2 was calculated and it is given in Table 2. From Table 2, it can be seen that ΔG_{bind} of Comp1 and Comp2 was found to be −35.094 and −32.796 Kcal/mol respectively. High negative ΔG_{bind} explains more affection towards the receptor cavity. Both molecules were found to have high negative ΔG_{bind} which clearly suggested that Comp1 and Comp2 might be potent CDK2 inhibitors.

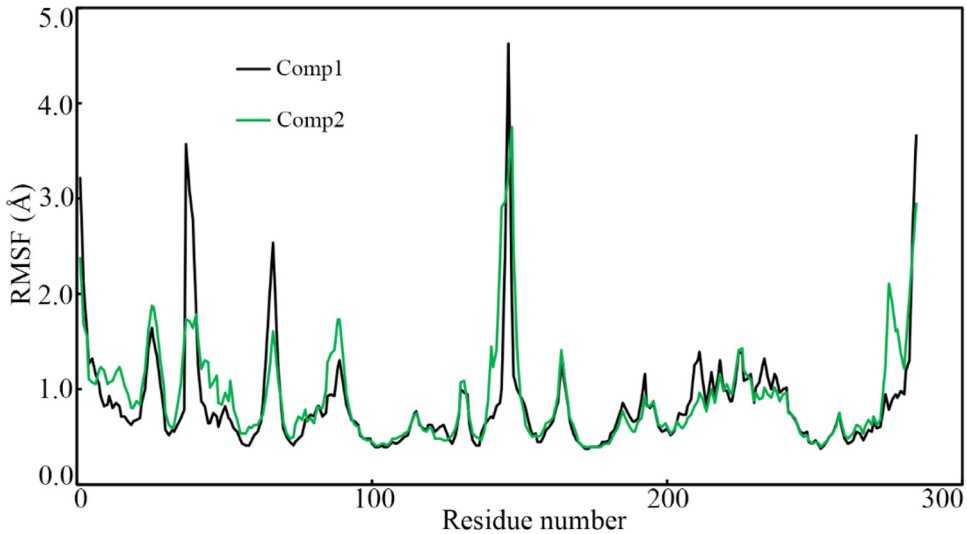

Fig. 5. RMSF of CDK2 amino acid residues bound with Comp1 and Comp2.

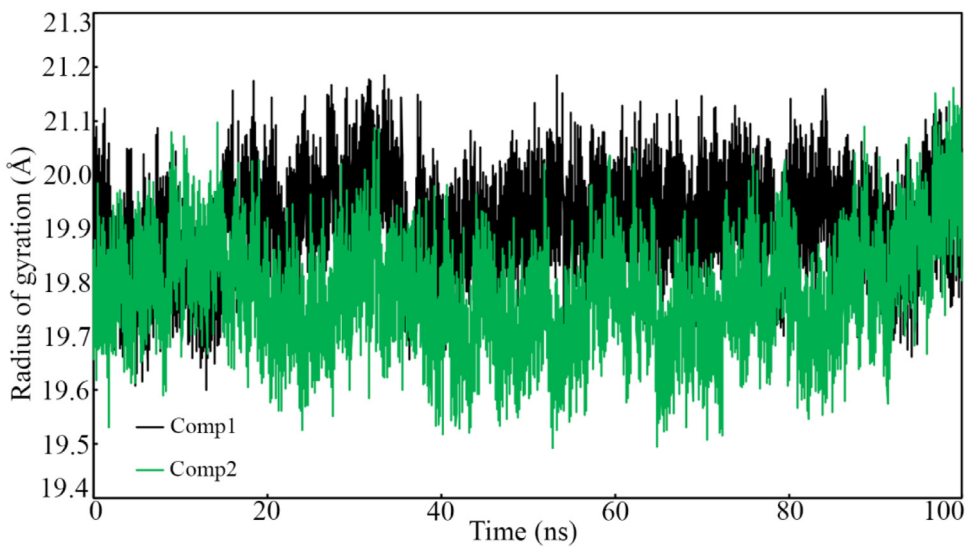

Fig. 6. Radius of gyration of CDK2 bound with Comp1 and Comp2.

4. Conclusion

The grinding technique has been used in this work to reduce the energy consumption and chemical additives and, more importantly, the reduction of environmental impacts relative to prepare thiazolidinone compounds. The grinding-mediated synthesis for two thiazolidinone derivatives exhibits high yields. Characteristics of the final product including ^{1}H NMR, ^{13}C NMR, GC-Mass, HRMS, CHNS indicate the configuration of the required compounds. Further, *in-silico* analyses of both molecules in the CDK2 protein was assessed. The molecular docking study was explained that both molecules potential enough to form a number of binding interactions with the catalytic amino residues of CDK2. Best docked pose of each molecule was further considered for 100 ns MD simulations study to explore the dynamic behavior of Comp1 and Comp2. The CDK2 backbone RMSD, residue RMSF, ligand RMSD and RoG obtained from MD simulation trajectories were clearly indicated that both molecules capable to retained inside the CDK2 receptor cavity. The binding affinity of Comp1 and Comp2 was checked by calculating the binding free energy from the ensemble of MD simulation trajectory. High negative binding energy suggested that both molecules possessed strong affections towards the CDK2. Therefore, it can be concluded that synthesized molecules might be crucial pharmaceutical chemical agents subjected to further experimental validation.

Declaration of Competing Interest

Authors declare that there is no competing interest

CRediT authorship contribution statement

Jasim Ali Abdullah: Conceptualization, Methodology. **Bilal J M Aldahham:** Methodology, Software, Validation, Formal analysis, Investigation, Writing - original draft, Project administration. **Muwafaq Ayesh Rabeea:** Conceptualization, Investigation, Writing - original draft, Writing - review & editing. **Fatmah Ali Asmary:** Validation, Formal analysis, Project administration. **Hassna Mohammed Alhajri:** Software, Investigation. **Md Ataul Islam:** Software, Validation, Writing - original draft, Writing - review & editing.

Acknowledgement

The authors extend their appreciation to the Deanship of Scientific Research at King Saud University for funding this work through research group No (RG-1441-430).

Supplementary materials

Supplementary material associated with this article can be found, in the online version, at doi:10.1016/j.molstruc.2020.129311.

References

[1] S.V. H.ote, S.P. Bhoyar, Heterocyclic compound: a review, IOSR J. Appl. Chem. 2014 (2014) 43–46.
[2] D.V. Andreeva, A.S. Tikhomirov, L.G. Dezhenkova, D.N. Kaluzhny, O.K. Mamaeva, S.E. Solovyova, Y.B. Sinkevich, A.E. Shchekotikhin, Heterocyclic analogs of 5,12-naphthacenequinone 16*. Synthesis and properties of new DNA ligands based on 4,11-diaminoanthra[2,3-b]thiophene-5,10-dione, Chem. Heterocycl. Compd. 56 (2020) 727–733. https://doi.org/10.1007/s10593-020-02723-3.
[3] D.M. Patel, H.M. Patel, Trimethylglycine-betaine-based-catalyst-promoted novel and ecocompatible pseudo-four-component reaction for regioselective synthesis of functionalized 6,8-dihydro-1′ H,5 H-spiro[[1,3]dioxolo[4,5- g]quinoline-7,5′-pyrimidine]-2′,4′,6′(3′ H)-trione derivati, ACS Sustain. Chem. Eng. 7 (2019) 18667–18676. https://doi.org/10.1021/acssuschemeng.9b05184.
[4] A.A. Al-Amiery, A.Y. Musa, A.A.H. Kadhum, A.B. Mohamad, The use of umbelliferone in the synthesis of new heterocyclic compounds, Molecules. 16 (2011) 6833–6843. https://doi.org/10.3390/molecules16086833.
[5] I. Orhan, B. Özcelik, B. Şener, Antiviral and antimicrobial evaluation of some heterocyclic compounds from Turkish plants, (2007) 303–323. https://doi.org/10.1007/7081_2007_072.
[6] R.M. Vala, D.M. Patel, M.G. Sharma, H.M. Patel, Impact of an aryl bulky group on a one-pot reaction of aldehyde with malononitrile and: N-substituted 2-cyanoacetamide, RSC Adv. 9 (2019) 28886–28893. https://doi.org/10.1039/c9ra05975j.
[7] D.M. Patel, R.M. Vala, M.G. Sharma, D.P. Rajani, H.M. Patel, A practical green visit to the functionalized [1,2,4]triazolo[5,1-b]quinazolin-8(4H)one scaffolds using the group-assisted purification (GAP) chemistry and their pharmacological testing, ChemistrySelect. 4 (2019) 1031–1041. https://doi.org/10.1002/slct.201803605.
[8] D.M. Patel, M.G. Sharma, R.M. Vala, I. Lagunes, A. Puerta, J.M. Padrón, D.P. Rajani, H.M. Patel, Hydroxyl alkyl ammonium ionic liquid assisted green and one-pot regioselective access to functionalized pyrazolodihydropyridine core and their pharmacological evaluation, Bioorg. Chem. 86 (2019) 137–150. https://doi.org/10.1016/j.bioorg.2019.01.029.
[9] P.J. Borpatra, B. Deka, M.L. Deb, P.K. Baruah, Recent advances in intramolecular C-O/C-N/C-S bond formation: via C-H functionalization, Org. Chem. Front. 6 (2019) 3445–3489. https://doi.org/10.1039/c9qo00863b.
[10] D. Havrylyuk, O. Roman, R. Lesyk, Synthetic approaches, structure activity relationship and biological applications for pharmacologically attractive pyrazole/pyrazoline-thiazolidine-based hybrids, Eur. J. Med. Chem. 113 (2016) 145–166. https://doi.org/10.1016/j.ejmech.2016.02.030.
[11] M.G. Sharma, R.M. Vala, D.M. Patel, I. Lagunes, M.X. Fernandes, J.M. Padrón, V. Ramkumar, R.L. Gardas, H.M. Patel, Anti-proliferative 1,4-dihydropyridine and pyridine derivatives synthesized through a catalyst-free, one-pot multicomponent reaction, ChemistrySelect. 3 (2018) 12163–12168. https://doi.org/10.1002/slct.201802537.
[12] G.C. Dos Santos, V.F. Moreno, B.H.S.T. Da Silva, L.C. Da Silva-Filho, Heterocyclic anthrazoline derivatives: a critical review, New J. Chem. 43 (2019) 18415–18432. https://doi.org/10.1039/c9nj04995a.
[13] R. Sadashiva, D. Naral, J. Kudva, S. Madan Kumar, K. Byrappa, R. Mohammed Shafeeulla, M. Kumsi, Synthesis, structure characterization, in vitro and in silico biological evaluation of a new series of thiazole nucleus integrated with pyrazoline scaffolds, J. Mol. Struct. 1145 (2017) 18–31. https://doi.org/10.1016/j.molstruc.2017.05.066.
[14] W. Li, J. Zhang, J. He, L. Xu, L. Vaccaro, P. Liu, Y. Gu, I2/DMSO-catalyzed transformation of N-tosylhydrazones to 1,2,3-thiadiazoles, Front. Chem. 8 (2020) 2–11. https://doi.org/10.3389/fchem.2020.00466.
[15] D. Havrylyuk, B. Zimenkovsky, O. Vasylenko, A. Gzella, R. Lesyk, Synthesis of new 4-thiazolidinone-, pyrazoline-, and isatin-based conjugates with promising antitumor activity, J. Med. Chem. 55 (2012) 8630–8641. https://doi.org/10.1021/jm300789g.
[16] G.K. Nampurath, S.P. Mathew, V. Khanna, R.T. Zachariah, S. Kanji, M.R. Chamallamudi, Assessment of hypolipidaemic activity of three thiazolidin-4-ones in mice given high-fat diet and fructose, Chem. Biol. Interact. 171 (2008) 363–368. https://doi.org/10.1016/j.cbi.2007.10.006.
[17] V.A. Shiryaev, Y.N. Klimochkin, Heterocyclic inhibitors of viroporins in the design of antiviral compounds, Chem. Heterocycl. Compd. 56 (2020) 626–635. https://doi.org/10.1007/s10593-020-02712-6.
[18] A. Gupta, R. Singh, P.K. Sonar, S.K. Saraf, Novel 4-thiazolidinone derivatives as anti-infective agents: synthesis, characterization, and antimicrobial evaluation, Biochem. Res. Int. 2016 (2016) 1–9. https://doi.org/10.1155/2016/8086762.
[19] O.M. Abdelhafez, K.M. Amin, H.I. Ali, M.M. Abdalla, R.Z. Batran, Synthesis of new 7-oxycoumarin derivatives as potent and selective monoamine oxidase A inhibitors, J. Med. Chem. 55 (2012) 10424–10436. https://doi.org/10.1021/jm301014y.
[20] A. Adhikari, B. Kalluraya, K.V. Sujith, K. Gouthamchandra, R. Mahmood, Microwave assisted synthesis of novel thiazolidinone analogues as possible bioactive agents, J. Adv. Res. 3 (2012) 325–330. https://doi.org/10.1016/j.jare.2011.10.003.
[21] M.M. Kut, M.Y. Onysko, [InlineMediaObject not available: see fulltext.] aryltellurium trihalides in the synthesis of heterocyclic compounds (microreview), Chem. Heterocycl. Compd. 56 (2020) 503–505. https://doi.org/10.1007/s10593-020-02688-3.
[22] S.K. Ramadan, E.A.E. El-Helw, Efficient microwave-assisted synthesis of some N-heterocycles integrated with a pyrazole moiety, Russ. J. Org. Chem. 55 (2019) 1626–1628. https://doi.org/10.1134/S1070428019100282.
[23] S.N. Shelke, G.R. Mhaske, V.D.B. Bonifácio, M.B. Gawande, Green synthesis and anti-infective activities of fluorinated pyrazoline derivatives, Bioorganic Med. Chem. Lett. 22 (2012) 5727–5730. https://doi.org/10.1016/j.bmcl.2012.06.072.
[24] A.R. Leman, E. Noguchi, Cell cycle regulation during viral infection, Methods Mol. Biol. 1170 (2014) 539–547. https://doi.org/10.1007/978-1-4939-0888-2.
[25] S. Tadesse, A.T. Anshabo, N. Portman, E. Lim, W. Tilley, C.E. Caldon, S. Wang, Targeting CDK2 in cancer: challenges and opportunities for therapy, Drug Discov. Today. 25 (2020) 406–413. https://doi.org/10.1016/j.drudis.2019.12.001.
[26] M. Kawakami, L.M. Mustachio, J. Rodriguez-Canales, B. Mino, J. Roszik, P. Tong, J. Wang, J.J. Lee, J.H. Myung, J.V. Heymach, F.M. Johnson, S. Hong, L. Zheng, S. Hu, P.A. Villalobos, C. Behrens, I. Wistuba, S. Freemantle, X. Liu, E. Dmitrovsky, Next-generation CDK2/9 inhibitors and anaphase catastrophe in lung cancer, J. Natl. Cancer Inst. 109 (2017) 1–11. https://doi.org/10.1093/jnci/djw297.
[27] J. Wang, T. Yang, G. Xu, H. Liu, C. Ren, W. Xie, M. Wang, Cyclin-dependent kinase 2 promotes tumor proliferation and induces radio resistance in glioblastoma, Transl. Oncol. 9 (2016) 548–556. https://doi.org/10.1016/j.tranon.2016.08.007.
[28] X. Yin, J. Yu, Y. Zhou, C. Wang, Z. Jiao, Z. Qian, H. Sun, B. Chen, Identification of CDK2 as a novel target in treatment of prostate cancer, Futur. Oncol. 14 (2018) 709–718. https://doi.org/10.2217/fon-2017-0561.
[29] G.M.E. Ali, D.A. Ibrahim, A.M. Elmetwali, N.S.M. Ismail, Design, synthesis and biological evaluation of certain CDK2 inhibitors based on pyrazole and pyrazolo[1,5-a] pyrimidine scaffold with apoptotic activity, Bioorg. Chem. 86 (2019) 1–14. https://doi.org/10.1016/j.bioorg.2019.01.008.
[30] F. Kilchmann, M.J. Marcaida, S. Kotak, T. Schick, S.D. Boss, M. Awale, P. Gönczy, J.L. Reymond, Discovery of a selective aurora A kinase inhibitor by virtual screening, J. Med. Chem. 59 (2016) 7188–7211. https://doi.org/10.1021/acs.jmedchem.6b00709.
[31] C.J.R. Bataille, M.B. Brennan, S. Byrne, S.G. Davies, M. Durbin, O. Fedorov, K.V.M. Huber, A.M. Jones, S. Knapp, G. Liu, A. Nadali, C.E. Quevedo, A.J. Russell, R.G. Walker, R. Westwood, G.M. Wynne, Thiazolidine derivatives as potent and selective inhibitors of the PIM kinase family, Bioorganic Med. Chem. 25 (2017) 2657–2665. https://doi.org/10.1016/j.bmc.2017.02.056.
[32] G. Koch, Medicinal chemistry, Chimia (Aarau). 71 (2017) 643. https://doi.org/10.2307/j.ctvnwc0d0.18.
[33] A.M. Senderowicz, Flavopiridol: the first cyclin-dependent kinase inhibitor in human clinical trials, Invest. New Drugs. (1999). https://doi.org/10.1023/A:1006353008903.
[34] C. Benson, J. White, J. De Bono, A. O'Donnell, F. Raynaud, C. Cruickshank, H. McGrath, M. Walton, P. Workman, S. Kaye, J. Cassidy, A. Gianella-Borradori, I. Judson, C. Twelves, A phase I trial of the selective oral cyclin-dependent kinase inhibitor seliciclib (CYC202; R-Roscovitine), administered twice daily for 7 days every 21 days, Br. J. Cancer. (2007). https://doi.org/10.1038/sj.bjc.6603509.
[35] M.M. Mita, A.C. Mita, J.L. Moseley, J. Poon, K.A. Small, Y.M. Jou, P. Kirschmeier, D. Zhang, Y. Zhu, P. Statkevich, K.K. Sankhala, J. Sarantopoulos, J.M. Cleary, L.R. Chirieac, S.J. Rodig, R. Bannerji, G.I. Shapiro, Phase 1 safety, pharmacokinetic and pharmacodynamic study of the cyclin-dependent kinase inhibitor dinaciclib administered every three weeks in patients with advanced malignancies, Br. J. Cancer. (2017). https://doi.org/10.1038/bjc.2017.288.
[36] W.G. Tong, R. Chen, W. Plunkett, D. Siegel, R. Sinha, R.D. Harvey, A.Z. Badros, L. Popplewell, S. Coutre, J.A. Fox, K. Mahadocon, T. Chen, P. Kegley, U. Hoch, W.G. Wierda, Phase I and pharmacologic study of SNS-032, a potent and selective Cdk2, 7, and 9 inhibitor, in patients with advanced chronic lymphocytic leukemia and multiple myeloma, J. Clin. Oncol. (2010). https://doi.org/10.1200/JCO.2009.26.1347.
[37] E.X. Chen, S. Hotte, H. Hirte, L.L. Siu, J. Lyons, M. Squires, S. Lovell, S. Turner, L. McIntosh, L. Seymour, A Phase i study of cyclin-dependent kinase inhibitor, AT7519, in patients with advanced cancer: NCIC Clinical Trials Group IND 177, Br. J. Cancer. (2014). https://doi.org/10.1038/bjc.2014.565.
[38] S. Aspeslagh, K. Shailubhai, R. Bahleda, A. Gazzah, A. Varga, A. Hollebecque, C. Massard, A. Spreafico, M. Reni, J.C. Soria, Phase I dose-escalation study of milciclib in combination with gemcitabine in patients with refractory solid tumors, Cancer Chemother. Pharmacol. (2017). https://doi.org/10.1007/s00280-017-3303-z.
[39] G. Mariaule, P. Belmont, Cyclin-dependent kinase inhibitors as marketed anticancer drugs: where are we now? A short survey, Molecules. (2014). https://doi.org/10.3390/molecules190914366.
[40] J. Safaei-Ghomi, R. Masoomi, Grinding-induced synthesis of heterocyclic fullerene derivatives under solvent-free conditions, Chem. Heterocycl. Compd. 51 (2015) 39–43. https://doi.org/10.1007/s10593-015-1657-x.
[41] J. Kaur, A. Kumari, S.S. Chimni, Grinding assisted, column chromatography

free decarboxylative carbon-carbon bond formation: Greener synthesis of 3, 3-disubstituted oxindoles, Tetrahedron. 73 (2017) 802–808. https://doi.org/10.1016/j.tet.2016.12.070.
[42] A.S. Hussen, A.P. Pandey, A. Sharma, Mechanochemical- (Hand-Grinding-) assisted domino synthesis of fused pyran-spirooxindoles under solvent- and catalyst-free condition, ChemistrySelect. 3 (2018) 11505–11509. https://doi.org/10.1002/slct.201802344.
[43] K. Mohammadiannejad, R. Ranjbar-Karimi, F. Haghighat, Synthesis of new mixed-bistriarylmethanes and novel 3,4-dihydropyrimidin-2(1H)one derivatives, New J. Chem. 43 (2019) 5543–5550. https://doi.org/10.1039/C8NJ05845H.
[44] N.H. Metwally, N.M. Rateb, H.F. Zohdi, A simple and green procedure for the synthesis of 5-arylidene-4-thiazolidinones by grinding, Green Chem. Lett. Rev. 4 (2011) 225–228. https://doi.org/10.1080/17518253.2010.544330.
[45] S. Mutahir, M.A. Khan, I.U. Khan, M. Yar, M. Ashraf, S. Tariq, R. long Ye, B. jing Zhou, Organocatalyzed and mechanochemical solvent-free synthesis of novel and functionalized bis-biphenyl substituted thiazolidinones as potent tyrosinase inhibitors: SAR and molecular modeling studies, Eur. J. Med. Chem. 134 (2017) 406–414. https://doi.org/10.1016/j.ejmech.2017.04.021.
[46] A. Naqvi, M. Shahnawaaz, A.V. Rao, D.S. Seth, N.K. Sharma, Synthesis of schiff bases via environmentally benign and energy-efficient greener methodologies, E-J. Chem. 6 (2009) 75–79. https://doi.org/10.1155/2009/589430.
[47] P. Vicini, A. Geronikaki, K. Anastasia, M. Incerti, F. Zani, Synthesis and antimicrobial activity of novel 2-thiazolylimino-5-arylidene-4-thiazolidinones, Bioorganic Med. Chem. 14 (2006) 3859–3864. https://doi.org/10.1016/j.bmc.2006.01.043.
[48] A.J.O. Oleg Trott, A. Schroer, AutoDock vina: improving the speed and accuracy of docking with a new scoring function, efficient optimization, and multithreading, J. Comput. Chem. (2010). https://doi.org/10.1002/jcc.
[49] D.R. Anderson, M.J. Meyers, R.G. Kurumbail, N. Caspers, G.I. Poda, S.A. Long, B.S. Pierce, M.W. Mahoney, R.J. Mourey, M.D. Parikh, Benzothiophene inhibitors of MK2. Part 2: improvements in kinase selectivity and cell potency, Bioorganic Med. Chem. Lett. (2009). https://doi.org/10.1016/j.bmcl.2009.02.017.
[50] G. Morris, R. Huey, W. Linkstrom, M. Sanner, R. Belew, D. Goodsell, Olson, AutoDock4 and AutoDockTools4: automated docking with selective receptor flexibility, J. Comput. Chem. (2010). https://doi.org/10.1002/jcc.
[51] S. Salentin, S. Schreiber, V.J. Haupt, M.F. Adasme, M. Schroeder, PLIP: fully automated protein-ligand interaction profiler, Nucleic Acids Res. (2015). https://doi.org/10.1093/nar/gkv315.
[52] L.F. Song, T.S. Lee, C. Zhu, D.M. York, K.M. Merz, Using AMBER18 for relative free energy calculations, J. Chem. Inf. Model. (2019). https://doi.org/10.1021/acs.jcim.9b00105.
[53] P. Mark, L. Nilsson, Structure and dynamics of the TIP3P, SPC, and SPC/E water models at 298K, J. Phys. Chem. A. (2001). https://doi.org/10.1021/jp003020w.
[54] J.A. Maier, C. Martinez, K. Kasavajhala, L. Wickstrom, K.E. Hauser, C. Simmerling, ff14SB: improving the accuracy of protein side chain and backbone parameters from ff99SB, J. Chem. Theory Comput. (2015). https://doi.org/10.1021/acs.jctc.5b00255.
[55] A. Peramo, Solvated and generalised Born calculations differences using GPU CUDA and multi-CPU simulations of an antifreeze protein with AMBER, Mol. Simul. (2016). https://doi.org/10.1080/08927022.2016.1183000.
[56] H.C. Andersen, Rattle: a “velocity” version of the shake algorithm for molecular dynamics calculations, J. Comput. Phys. (1983). https://doi.org/10.1016/0021-9991(83)90014-1.
[57] D.R. Roe, T.E. Cheatham, PTRAJ and CPPTRAJ: software for processing and analysis of molecular dynamics trajectory data, J. Chem. Theory Comput. (2013). https://doi.org/10.1021/ct400341p.
[58] A. Onufriev, D. Bashford, D.A. Case, Exploring protein native states and large-scale conformational changes with a modified generalized born model, Proteins Struct. Funct. Bioinforma. 55 (2004) 383–394. https://doi.org/10.1002/prot.20033.
[59] J. Weiser, P.S. Shenkin, W.C. Still, Approximate atomic surfaces from linear combinations of pairwise overlaps (LCPO), J. Comput. Chem. 20 (1999) 217–230. https://doi.org/10.1002/(SICI)1096-987X(19990130)20:2⟨217::AID-JCC4⟩3.0.CO;2-A.
[60] C. Ainsworth, The principles of heterocyclic chemistry, J. Chem. Educ. 46 (1969) A201. https://doi.org/10.1021/ed046pa201.2.
[61] K.A. Thorn, 13C and 15N NMR identification of product compound classes from aqueous and solid phase photodegradation of 2,4,6-trinitrotoluene, 2019. https://doi.org/10.1371/journal.pone.0224112.
[62] H.X. Pang, Y.H. Hui, K. Fan, X.J. Xing, Y. Wu, J.H. Yang, W. Shi, Z.F. Xie, A catalysis study of mesoporous MCM-41 supported Schiff base and CuSO4•5H2O in a highly regioselective synthesis of 4-thiazolidinone derivatives from cyclocondensation of mercaptoacetic acid, Chinese Chem. Lett. 27 (2016) 335–339. https://doi.org/10.1016/j.cclet.2015.10.029.
[63] S. Genheden, U. Ryde, The MM/PBSA and MM/GBSA methods to estimate ligand-binding affinities, Expert Opin. Drug Discov. (2015). https://doi.org/10.1517/17460441.2015.1032936.
[64] T. Hou, J. Wang, Y. Li, W. Wang, Assessing the performance of the MM/PBSA and MM/GBSA methods. 1. The accuracy of binding free energy calculations based on molecular dynamics simulations, J. Chem. Inf. Model. (2011). https://doi.org/10.1021/ci100275a.
[65] S. Bhowmick, N.A. AlFaris, J.Z. ALTamimi, Z.A. ALOthman, T.S. Aldayel, S.M. Wabaidur, M.A. Islam, Screening and analysis of bioactive food compounds for modulating the CDK2 protein for cell cycle arrest: multi-cheminformatics approaches for anticancer therapeutics, J. Mol. Struct. (2020). https://doi.org/10.1016/j.molstruc.2020.128316.